

# Pore-scale study on interfacial characteristic of CO<sub>2</sub>-oil-glass beads during CO<sub>2</sub>-EOR

Xin Wang<sup>1</sup>, Jilong Zheng<sup>2,3</sup>, Shaohua Li<sup>1</sup>, Pengfei Lv<sup>4</sup>, Lanlan Jiang<sup>1,\*</sup>, Yongchen Song<sup>1</sup>

1 Key Laboratory of Ocean Energy Utilization and Energy Conservation of Ministry of Education, Dalian University of Technology, Dalian, 116024, China

2 Clean Energy Branch of CNOOC Energy Development Co., Ltd., Tianjin, 300452, China

3 Survey&Design Co., Ltd.CONHW, Zhanjiang, 524000, China

4 School of Energy and Power Engineering, North University of China, Taiyuan, Shanxi, 030051, China

(\*Corresponding Author: lanlan@dlut.edu.cn)

## ABSTRACT

CO<sub>2</sub>-EOR (Enhanced Oil Recovery) is a vital method to increase oil recovery while significantly lower greenhouse gas emissions. The near-miscible conditions are useful to improve displacement efficiency and oil recovery by CO<sub>2</sub> injection. In this study, at the near-miscible condition of 8MPa, 40°C, using X-ray micro-tomography (micro-CT), pore-scale interfacial characteristics can be obtained in the CO<sub>2</sub>-oil-glass beads system, such as wettability, which represents the tendency of fluids in the solid. A displacement of oil by CO<sub>2</sub> was performed to examine the two-phase interfacial characteristics in the gas-oil-solid system. With the multi-phase identification approach and in-situ spatial distribution of contact angle ( $\theta$ ), the  $\theta$  at 5.5PV was nearly 66.99° at near-miscible conditions, which indicates an intermediate-wet system. With increasing injection pore volumes (PV) from 5.5PV to 16.4PV, the contact angle increases from 66.99° to 70.42°, indicating a decrease in the water-wet property. Although oil resides in pores of all sizes (big, medium, and small), gas often fills the larger pores. The interfacial curvature examination revealed that in-situ capillary pressure provides a distribution with an average value near zero. The rock performed a wettability reversal from a water-wet to an intermediate-wet condition. The knowledge of near-miscible two-phase flow is helpful to enhance oil recovery and storage efficiency.

**Keywords:** CCUS, pore-scale, wettability, interfacial property, micro-CT

## NONMENCLATURE

### Abbreviations

EOR	Enhanced Oil Recovery
Micro-CT	X-ray micro-tomography
PV	pore volume
FOV	field of view
PNM	pore network model

### Symbols

$\theta$	contact angle
$S_{CO_2}$	CO <sub>2</sub> saturation

## 1. INTRODUCTION

EOR (Enhanced Oil Recovery) is a vital method to increase oil recovery while significantly lower greenhouse gas emissions<sup>[1]</sup>, usually performed in experimental studies<sup>[2]</sup>, numerical simulation<sup>[3]</sup>, and site tests<sup>[4]</sup>. CO<sub>2</sub> injection is frequently used in oil recovery<sup>[5]</sup>. Fluid parameters and interfacial characteristics may have an impact on oil recovery<sup>[6, 7]</sup>. In order to comprehend the interactions and mechanisms in the CO<sub>2</sub>-EOR system, it is critical to grasp the interfacial feature.

Wettability is a crucial interfacial property that represents the fluids' affinity in porous media<sup>[8]</sup>. Zankoor et al.<sup>[9]</sup> achieved a geometric analysis of the fluid-fluid-rock interface at the pore scale by in-situ capillary pressure and wettability, which showed an agreement between the image-based capillary pressure and macroscopic measurements in multiphase flow. Jahanbakhsh et al.<sup>[10]</sup> demonstrated that heterogeneous

wettability had an impact on fluid interface evolution and displacement patterns. There are various studies to investigate the influence of wettability on oil recovery. Theoretically, oil recovery is higher in more water-wet conditions<sup>[5, 11]</sup>. High tertiary oil recovery can be achieved through wettability reversal<sup>[12]</sup>. Zhao et al.<sup>[13]</sup> discovered that in the uniformly-wet system, oil recovery increased as the system was less water-wet, while in the mixed-wet situation, the greatest recovery occurred at a tiny fraction of water-wet conditions. The impact of wettability on EOR ought to be examined for more investigations.

The development of X-ray microtomography (micro-CT) has made it possible to monitor three-dimensional (3D) fluid flow and migration at pore-scale<sup>[14]</sup>. In the CO<sub>2</sub>/oil-brine-rock systems, several experimental studies have carried out the pore-scale wettability measurements by micro-CT<sup>[15-17]</sup>. The wettability also has an impact on the fluid-fluid interfacial curvature, which is another measure of the interfacial properties<sup>[18]</sup>. The interfacial phenomena in the CO<sub>2</sub>-oil-glass beads system at near-miscible conditions, particularly at the pore size, is still not fully understood.

In this study, we conduct a near-miscible experiment at high pressures and temperatures (8MPa, 40°C) in a water-wet sample. To observe the wettability at near-miscible conditions, we study (i) pore characteristics, (ii) in-situ wettability, (iii) interfacial curvature, and (iv) capillary pressure.

## 2. MATERIAL AND METHODS

### 2.1 Experimental setup and materials

The core was made 6 mm in diameter and 30 mm in length and filled with BZ-1 (purchased from As-One Co., Ltd. in Japan) for use. In the near-miscible injection studies, the fluid phases were (i) scCO<sub>2</sub> as the non-wetting injection and (ii) N-hexane as the wetting injection. To increase contrast in the micro-CT images, 10%wt 1-Iodobutaneto solution was added to the oil. The experiment was conducted at 40°C and 8MPa, we fitted a linear regression line and deduced the interfacial tension at the given gas-oil conditions.

The experimental system was made up of a micro-CT system and a core displacement system. A CT scanner, a computer, and an image display system make up the micro-CT system. The CT scanner may display numerous experimental results based on various object properties when using X-rays to scan the objects. As the computer extracts the data from the scanned images, the image

display system exhibits the reconstructed CT images. Two ISCO pumps, a core holder, a backpressure pump, a vacuum pump, two pressure transducers, and a confining pressure pump are the components of the core displacement system. The ISCO pumps are used to inject oil and CO<sub>2</sub>. The core holder's PEEK material enables X-rays to penetrate through and provide precise images. A diagram of the CO<sub>2</sub>-oil displacement process is shown in Fig. 1.

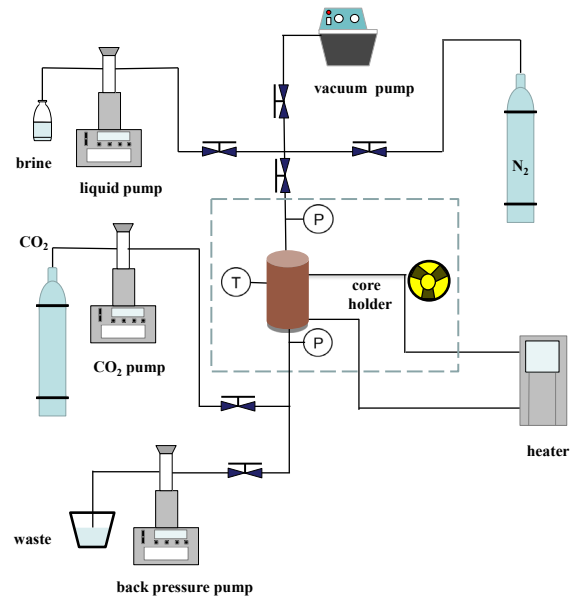


Fig. 1. Schematic diagram of CO<sub>2</sub>-oil displacement in micro-CT system.

### 2.2 Experimental procedures

The experiment processes are as follows:

(1) The CT values of CO<sub>2</sub>, oil, and solid are obtained at scanning voltage and current of 110kV and 70A, respectively. The experimental pressure is 8MPa, and the temperature is fixed at 40°C.

(2) After putting the BZ-1 in the core holder, pressurize it to an experimental confining pressure and backpressure. Then, vacuum it to a steady state, or until there is no noticeable change in the pressure within 2 hours.

(3) To achieve a stable state, the core is vacuumed for 7 days before being saturated with oil for 21 days at 8 MPa. The oil-filled core is scanned to determine the CT value at each scanning interval.

(4) Close the outlet valve and pressurize CO<sub>2</sub> at the inlet using the injection pump. The confining pressure is adjusted to be 2MPa greater than the inlet pressure. The injection pump stops when the desired inlet pressure is reached, and the inlet valve is then closed. The

backpressure regulator continuously monitors for indications of liquid flow.

### 2.3 Image Processing

For simple observation and contrast evaluation, all of the three-dimensional CT data were reconstructed, and the images were processed using Avizo. A non-local means edge filter was utilized to reduce image noise<sup>[19]</sup>. We performed a topological assessment of the three-phase system by extracting a small cubic subvolume with the dimensions 300×300×604 voxels. Fluid saturations, local wettability of positions and injection pore volumes, fluid-solid interfacial areas, curvatures, and capillary pressure were determined for each subvolume. The watershed segmentation method was used to obtain different phases of the CT data and the triple lines can be generated with the surface of different phases. To create a plane perpendicular to the triple contact line, an orthogonal plane was rotated and the contact angle between the CO<sub>2</sub>/oil and oil/solid interfaces at the triple contact point was calculated on the plane<sup>[15]</sup>. The complete process is shown in Fig. 2.

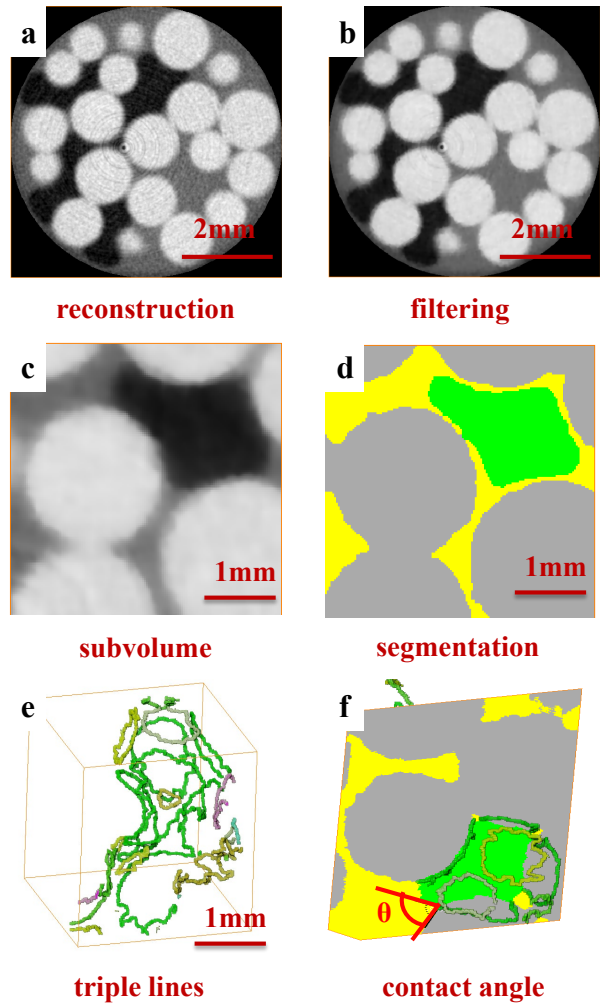


Fig.2. A procedure for image process. (a) The reconstructed picture. Rock is the lightest phase, CO<sub>2</sub> the darkest phase, and oil the middle phase. (b) The image after a non-local means filter. (c) A subsection of the volume. (d) The image after watershed segmentation. (e) The triple contact line extraction algorithm (f) The contact angle at a three-phase point.

## 3. RESULTS AND DISCUSSION

### 3.1 Pore and throat parameters

Pore structure studies are essential to investigate the displacement mechanism and phase distribution. The basic physical properties—like porosity, pore radius distribution, and throat distribution—are discussed in this section. The pore space was composed of CO<sub>2</sub> and oil to calculate the phase saturation and pore characteristics of the core sample. Fig. 3 illustrates the porosity distribution over the Field of View (FOV) after 604 slices from the tomograms were obtained, each of the slice's porosity was determined. The mean porosity was 0.284, and the variance in the porosity was 2.71%. The pore

network model (PNM) was applied to analyze 230 pores connected to 524 throats in the subvolume. Using the calculation of the parameters of pores and throats, the sample had an average pore and throat radius of 258.39 $\mu\text{m}$  and 136.92 $\mu\text{m}$ , respectively.

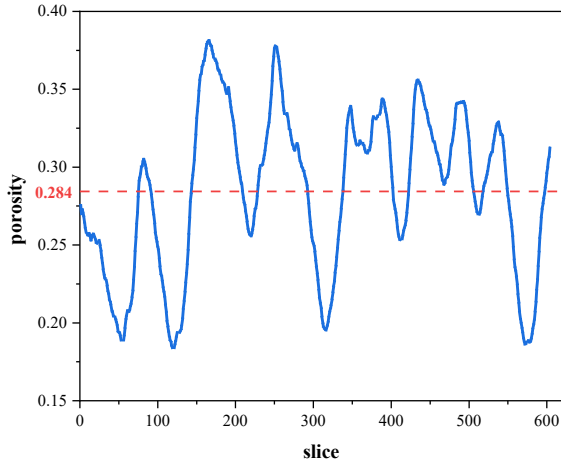


Fig. 3. The porosity distribution of each slice in BZ-1.

### 3.2 In-situ wettability distribution

Wettability is usually characterized by the contact angle in the fluid-fluid-solid system. Due to the emergence of an oil layer around the gas phase in immiscible conditions, the gas-oil contact angle should be close to zero. Low gas-oil interfacial tensions, also referred to as near-miscible conditions, cause gas and oil to become equivalent as they get close to being miscible. In situations where the contact angle between gas and oil and water is the same, the preference for gas and oil on the surface is almost identical<sup>[20]</sup>. With the multi-phase extraction technique method, we manually calculated approximately 100 angles in the contact lines. Fig. 4 depicts the distributions of local contact angles during drainage and reveals a wide range associated with heterogeneity, surface roughness, and topology. With the Gauss fit method, the mean contact angle was 66.99° at 5.5 PV and exhibited a preference for coating by oil over gas on the rock surface because gas is more non-wetting than oil. As injection pore volumes (PV) increases to 16.4PV, the contact angle increases to 70.42°, indicating a gradual decrease of the sample's water-wet property. A relatively large gas-oil contact angle of 72.50° was formed at 33.1V, demonstrating that gas and oil were almost equally wet to the surface. Additionally, contact angles varied in different positions, demonstrating the non-uniform wettability of the sample.

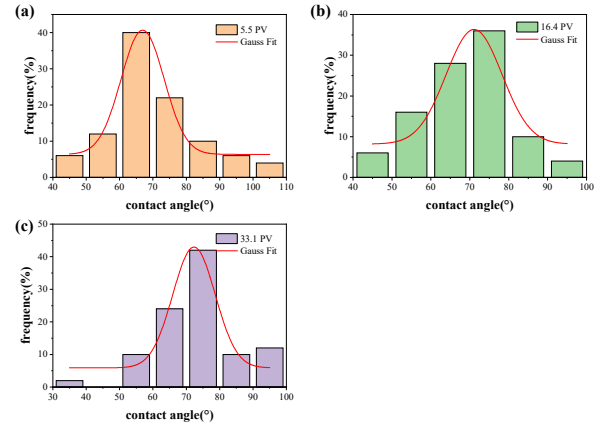


Fig. 4. The local contact angle distributions of 5.5PV, 16.4PV, and 33.1PV.

### 3.3 Capillary pressure

Capillary pressure (the difference in pressure between the wetting and non-wetting phases), which is regulated by pore radius, wettability, and interfacial tension<sup>[21]</sup>, is the main mechanism for CO<sub>2</sub>-oil displacement. We quantified the local in-situ capillary pressure using pore-scale fluid occupancy maps to study the displacement behaviors. In the experiment, the CO<sub>2</sub>-oil interface was generated and smoothed for imaging. A curvature analysis of the interface between the non-wetting and wetting phases was carried out by generally modeling the surface as a quadratic form. The mean interfacial curvature between two phases was used to compute the capillary pressure by the Young-Laplace equation.

$$P_c = 2\sigma\kappa \quad (1)$$

where  $\sigma$  is the interfacial tension,  $\kappa$  is the mean interfacial curvature (i.e., the average of the maximum and minimum curvature values of the surface). The interfacial curvature derived from the micro-CT images produced a distribution with the most positive values, which was consistent with the contact angle value below 90° representing the water-wet characteristics. The negative values are possible as a result of segmentation issues and poor imaging resolution. Fig. 5 shows the capillary pressure as a function of saturation for CO<sub>2</sub>-decane with an interfacial tension of 0.927mN/m at 8MPa, 40°C.

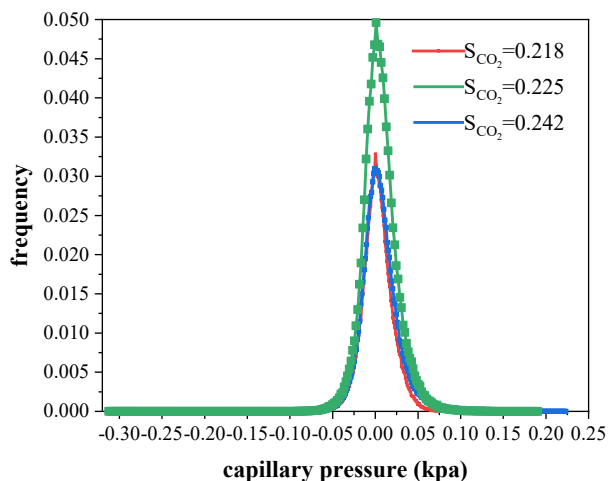


Fig. 5. Capillary pressure as a function of CO<sub>2</sub> saturation.

The near-miscible state is defined as the low CO<sub>2</sub>-oil interfacial tension,  $\leq 1\text{mN/m}$ , which results in a low capillary pressure between CO<sub>2</sub> and gas. According to the findings of Alhosani et al. (2021) [22], a lower capillary pressure can lead to a higher oil displacement efficiency. The tower-like local capillary pressure displayed a narrow distribution and a high value at zero capillary pressure using the interface curvature analysis. This corresponds to the in-situ measurement of nearly 90°, revealing that the interfaces became nearly flat with both curvatures approaching zero. The distributions of capillary pressure at various saturations were nearly identical showing that the effect of CO<sub>2</sub> saturation on capillary pressure was little.

#### 4. CONCLUSIONS

In a near-miscible CO<sub>2</sub>-oil displacement at 8 MPa and 40°C, we focused on the 3D pore-scale features, in-situ wettability, CO<sub>2</sub>-oil interfacial curvature, and capillary pressure.

The study's main conclusions are as follows:

1. The mean porosity is 0.284 in BZ-1, which is within the range of most rocks.
2. The average contact angle increases from 66.99° to 70.42° as injection pore volumes (PV) increases from 5.5PV to 16.4PV, indicating a gradual decrease of the sample's water-wet property. A relatively large gas-oil contact angle of 72.5° was formed after displacement, demonstrating that gas and oil were almost equally wet to the surface finally.
3. The CO<sub>2</sub>-oil interfacial curvature analysis revealed that in-situ capillary pressure produces a distribution with an average value close to zero. According to in-situ contact angle

measurements, the rock experienced a wettability reversal from a water-wet to an intermediate-wet condition. As the curvature went toward zero, the interfaces likewise became nearly flat.

#### ACKNOWLEDGEMENT

This study was supported by the National Natural Science Foundation of China (Grant 52176057 and Grant No. 52106213), Excellent Youth Foundation of Liaoning Province (Grant 2022YQ-12), Dalian youth science and technology star Project (Grant 2021RQ069), Fundamental Research Program of Shanxi Province (20210302124207), Shanxi Scholarship Council of China (2020-116). The study was also supported by Special Project for key Research and Development Program of Xinjiang Autonomous Region (Grant 2022B01033), the Key Laboratory of Gas Hydrate, Guangzhou Institute of Energy Conversion, Chinese Academy of Sciences (Grant E129kf1101), and the Fundamental Research Funds for the Central Universities (DUT22LAB103).

#### DECLARATION OF INTEREST STATEMENT

The authors declare that they have no known competing financial interests or personal relationships that could have appeared to influence the work reported in this paper. All authors read and approved the final manuscript.

#### REFERENCE

- [1] Hill L B, Li X, Wei N. CO<sub>2</sub>-EOR in China: A comparative review [J]. International Journal of Greenhouse Gas Control, 2020, 103.
- [2] Han J, Han S, Sung W, et al. Effects of CO<sub>2</sub> miscible flooding on oil recovery and the alteration of rock properties in a carbonate reservoir [J]. Journal of CO<sub>2</sub> Utilization, 2018, 28: 26-40.
- [3] Cui G, Zhang L, Tan C, et al. Injection of supercritical CO<sub>2</sub> for geothermal exploitation from sandstone and carbonate reservoirs: CO<sub>2</sub> –water–rock interactions and their effects [J]. Journal of CO<sub>2</sub> Utilization, 2017, 20: 113-128.
- [4] Lv G, Li Q, Wang S, et al. Key techniques of reservoir engineering and injection–production process for CO<sub>2</sub> flooding in China's SINOPEC Shengli Oilfield [J]. Journal of CO<sub>2</sub> Utilization, 2015, 11: 31-40.
- [5] Sheng J J. Modern chemical enhanced oil recovery: theory and practice [M]. Gulf Professional Publishing, 2010.

- [6] Agbalaka C C, Dandekar A Y, Patil S L, et al. The effect of wettability on oil recovery: A review; proceedings of the SPE Asia Pacific Oil and Gas Conference and Exhibition, F, 2008 [C]. OnePetro.
- [7] Anderson W. Wettability literature survey-part 2: Wettability measurement [J]. *Journal of petroleum technology*, 1986, 38(11): 1246-1262.
- [8] Donaldson E C, Thomas R D, Lorenz P B. Wettability Determination And Its Effect On Recovery Efficiency [J]. *Society of Petroleum Engineers Journal*, 1969, 9(1): 13-+.
- [9] Zankoor A, Khishvand M, Mohamed A, et al. In-situ capillary pressure and wettability in natural porous media: Multi-scale experimentation and automated characterization using X-ray images [J]. *J Colloid Interface Sci*, 2021, 603: 356-369.
- [10] Suzuki K, Miida H, Wada H, et al. Feasibility Study on CO<sub>2</sub> Micro-Bubble Storage (CMS) [J]. *Energy Procedia*, 2013, 37: 6002-6009.
- [11] Morrow N R J J o p t. Wettability and its effect on oil recovery [J]. 1990, 42(12): 1476-1484.
- [12] Donaldson E C, Alam W. *Wettability* [M]. Elsevier, 2013.
- [13] Zhao X, Blunt M J, Yao J. Pore-scale modeling: Effects of wettability on waterflood oil recovery [J]. *Journal of Petroleum Science and Engineering*, 2010, 71(3-4): 169-178.
- [14] Zou S, Sun C. X-ray microcomputed imaging of wettability characterization for multiphase flow in porous media: A review [J]. *Capillarity*, 2020, 3(3): 36-44.
- [15] Andrew M, Bijeljic B, Blunt M J. Pore-scale contact angle measurements at reservoir conditions using X-ray microtomography [J]. *Advances in Water Resources*, 2014, 68: 24-31.
- [16] Singh K, Bijeljic B, Blunt M J. Imaging of oil layers, curvature and contact angle in a mixed-wet and a water-wet carbonate rock [J]. *Water Resources Research*, 2016, 52(3): 1716-1728.
- [17] Alhammadi A M, AlRatrouf A, Singh K, et al. In situ characterization of mixed-wettability in a reservoir rock at subsurface conditions [J]. *Sci Rep*, 2017, 7(1): 10753.
- [18] Scanziani A, Singh K, Blunt M J, et al. Automatic method for estimation of in situ effective contact angle from X-ray micro tomography images of two-phase flow in porous media [J]. *J Colloid Interface Sci*, 2017, 496: 51-59.
- [19] Buades A, Coll B, Morel J-M. Nonlocal image and movie denoising [J]. *International journal of computer vision*, 2008, 76: 123-139.
- [20] Alhosani A, Scanziani A, Lin Q, et al. In situ pore-scale analysis of oil recovery during three-phase near-miscible CO<sub>2</sub> injection in a water-wet carbonate rock [J]. *Advances in Water Resources*, 2019, 134.
- [21] Qi S-C, Yu H-Y, Han X-B, et al. Countercurrent imbibition in low-permeability porous media: Non-diffusive behavior and implications in tight oil recovery [J]. *Petroleum Science*, 2023, 20(1): 322-336.
- [22] Alhosani A, Lin Q, Scanziani A, et al. Pore-scale characterization of carbon dioxide storage at immiscible and near-miscible conditions in altered-wettability reservoir rocks [J]. *International Journal of Greenhouse Gas Control*, 2021, 105.